Preprogrammed Long-Term Systemic Pulsatile Delivery of Parathyroid Hormone to Strengthen Bone

*Ming Dang, Amy J. Koh, Theodora Danciu, Laurie K. McCauley, and Peter X. Ma**

Parathyroid hormone (PTH) is the only US Food and Drug Administration (FDA)-approved anabolic agent for the treatment of osteoporosis. The anabolic action of PTH depends on the mode of PTH administration. Pulsatile administration promotes bone formation, however continuous PTH exposure results in bone resorption. In addition, the therapeutic effect of PTH is optimal when the dose and duration fit the therapeutic window. Current PTH treatment requires daily injection, which is neither a convenient nor a favorable choice of patients. Here, an implantable and biodegradable device capable of long-term pulsatile delivery of PTH is developed as a patient-friendly alternative. The advanced materials and fabrication techniques developed in this work enable us to preprogram a pulsatile delivery device to systemically deliver 21 daily pulses of PTH that build bone in vivo. In addition, the device is biodegradable and absorbable in vivo so that no retraction procedure is needed. Therefore, this implantable and biodegradable pulsatile device holds promise to promote bone growth and treat various conditions of bone loss without the burden of daily injections or secondary surgeries.

1. Introduction

Biological systems are intricately sensitive to the location and timing of physiological signals and therapeutics. For example, to eliminate pain or to correct an endocrine disorder, therapeutic drugs need to be delivered at specific time points and follow a certain pattern[1] of distribution. While researchers have made significant progress, the majority of drug delivery systems developed thus far aim to achieve a prolonged and sustained delivery of a required biological compound.[2] However, there has been limited progress in designing controlled release systems to couple the spatiotemporal sensitivity of a patient to a drug to enable or optimize its therapeutic effect.

Parathyroid hormone (PTH) is currently the only FDA-approved anabolic agent for the treatment of osteoporosis in the US,[3] however its anabolic or catabolic action depends on the pattern of PTH delivery. Intermittent (pulsatile) administration improves bone microarchitecture, mineral density, and strength, whereas continuous exposure of PTH leads to bone resorption.[4] Current intermittent PTH treatment requires daily subcutaneous injection, which is neither a convenient nor a favorable choice of patients.[5] Thus, there is a clear clinical need for a patient-friendly alternative treatment capable of pulsatile PTH delivery, which would improve patients' compliance and thereby their therapeutic outcome.

A variety of delivery strategies have been explored to achieve controlled release in a pulsatile manner from various platforms such as micelles,[6] liposomes,[7] micro/nanoparticles,[8] hydrogel,[9] and microchips.[10] Based on the triggering mechanisms, these pulsatile delivery systems can be classified into stimuli-responsive pulsatile release systems and self-regulated pulsatile release systems. In stimuli-responsive systems, drug carriers release the loaded drug when triggered by external stimuli[11] such as temperature,[12] pH,[13] light,[14,15] enzyme,[16] ultrasound,[17] biomolecules,[18] and electric[19] or magnetic fields.[20] These responsive systems can achieve pulsatile release but have also shown various limitations, such as an initial burst release, an irreversible triggered release, a short time interval (seconds to minutes), or a short release duration. Moreover, critical considerations have to be employed regarding the safety and biocompatibility of these responsive systems because many of the stimuli cannot be easily and safely utilized in patients and most of them are constructed with nondegradable polymers or inorganic materials.[15,21] Due to these limitations, few of them have been successfully implemented in patient care as a pulsatile PTH treatment. In self-regulated release systems, drugs are loaded in reservoirs sealed by a barrier material, which is usually composed of an erodible or biodegradable

M. Dang, Prof. P. X. Ma[+]
Macromolecular Science and Engineering Center
University of Michigan
Ann Arbor, MI 48109, USA
E-mail: mapx@umich.edu

A. J. Koh, Prof. T. Danciu, Prof. L. K. McCauley
Department of Periodontics and Oral Medicine
University of Michigan School of Dentistry
Ann Arbor, MI 48109, USA

Prof. L. K. McCauley
Department of Pathology
University of Michigan Medical School
Ann Arbor, MI 48109, USA

Prof. P. X. Ma
Department of Biomedical Engineering
University of Michigan
Ann Arbor, MI 48109, USA

Prof. P. X. Ma
Department of Materials Science and Engineering
The University of Michigan
Ann Arbor, MI 48109, USA

[+]Present address: Department of Biologic and Materials Sciences, The University of Michigan, 1011 North University Ave., Room 2209, Ann Arbor, MI 48109-1078, USA

DOI: 10.1002/adhm.201600901

polymer.[5,10,22] After the barrier material is eroded or degraded, drugs are rapidly released from the inner reservoir. The control over the pulsatile kinetics depends on the properties of the barrier materials and the design of the reservoir structure.

In addition to the pulsatile releasing feature, the ability of long-term release is also critically important in developing a PTH delivery system. A series of studies indicate the beneficial effects of intermittent PTH administration on bone,[23] and its prominent anabolic action during three weeks of exogenous administration in an in vivo osteoregeneration mouse model.[24] Six-week systemic PTH administration was further demonstrated to be beneficial to osseous regeneration in a clinical human study.[25] Therefore, a delivery system capable of long-term release is needed to cover the effective therapeutic window. Previously, we developed a self-regulated pulsatile delivery device and achieved daily release of bioactive PTH for 4 d.[5] However, due to its limited time frame, the device was not evaluated for its therapeutic function. The challenge lies in the structural design and fabrication techniques to enable a large number of controlled release pulses over a long duration. Ultimately, a biodegradable device that degrades and is absorbed in vivo without the need to be surgically removed is desirable.

Herein, the aim of this work was to develop an advanced patient-friendly delivery system, which would overcome the hindrances of the current treatment regimen (daily injection) and achieve the optimal anabolic effect with preprogrammed PTH delivery. We designed implantable and biodegradable polymeric devices using a surface erosion polyanhydride (PA) developed in our lab[26] and advanced fabrication techniques to achieve preprogrammed daily pulses for 21 d. We also developed a device, which achieved continuous PTH release over 21 d. Henceforth, the devices served as a platform that allowed us to study the distinct PTH delivery patterns (pulsatile vs continuous) and their systemic therapeutic effects on bone in a mouse model (**Figure 1**).

2. Results and Discussion

2.1. PTH Delivery Devices and Preprogrammed Pulsatile Releases

2.1.1. Pulsatile Delivery Device

We fabricated a multipulse PTH delivery device consisting of alternating drug layers and isolation layers via an electrostatic-assisted layer-by-layer stacking technique (**Figure 2**A). The isolation layer was made of biocompatible PA, which is biodegradable through surface erosion. Bovine serum albumin (BSA) (control protein) or PTH was mixed with alginate to form the drug layer. Alginate was used as the carrier because of its biocompatibility and processibility. We first investigated the surface potential of the two layers using Kelvin probe force microscopy (KPFM).[27] A PA or alginate-PTH layer was coated onto a gold substrate. The relative surface potentials of the two polymeric layers were calculated using the gold surface as reference (0 mV) (Figure S1A, Supporting Information). We found that the PA layer was positive and the drug layer was nearly neutral. The surface potential of the PA layer (≈40 mV) was about six times higher than that of the drug layer (≈7 mV) (Figure S1B,C, Supporting Information). The intrinsic surface potential difference facilitated the generation of opposite electrostatic charges on the two layers. We generated positive charges on the PA layer by rubbing it with a Telfon film that has a strong tendency to gain electrons. Conversely, we generated negative charges on the drug layer by rubbing it with a glass slide that has a strong tendency to lose electrons. The electrostatic voltages between the two different layers were measured with an electrostatic meter and the results indicated that we were able to generate opposite charges on the PA layer (≈+160 mV) and the drug layer (≈–80 mV) (Figure 2B). One positive PA layer and one negative drug layer were attracted to each other and formed a bilayer structure. The bilayers were

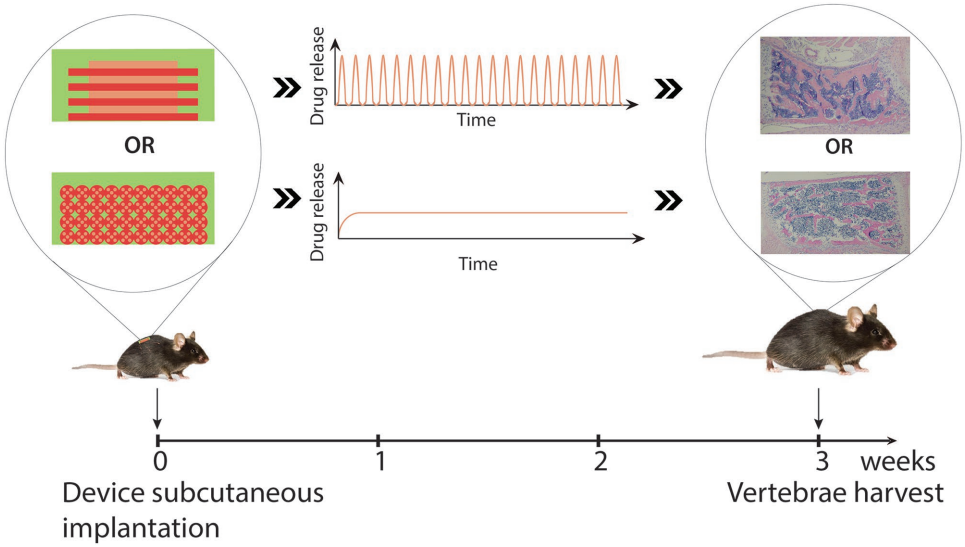

Figure 1. Experimental design used to investigate the therapeutic effects of PTH released from the pulsatile delivery device and the continuous delivery device. The PTH delivery devices were subcutaneously implanted in mice and bones and serum were collected three weeks later to examine the systemic effects of the two PTH release modes on bone.

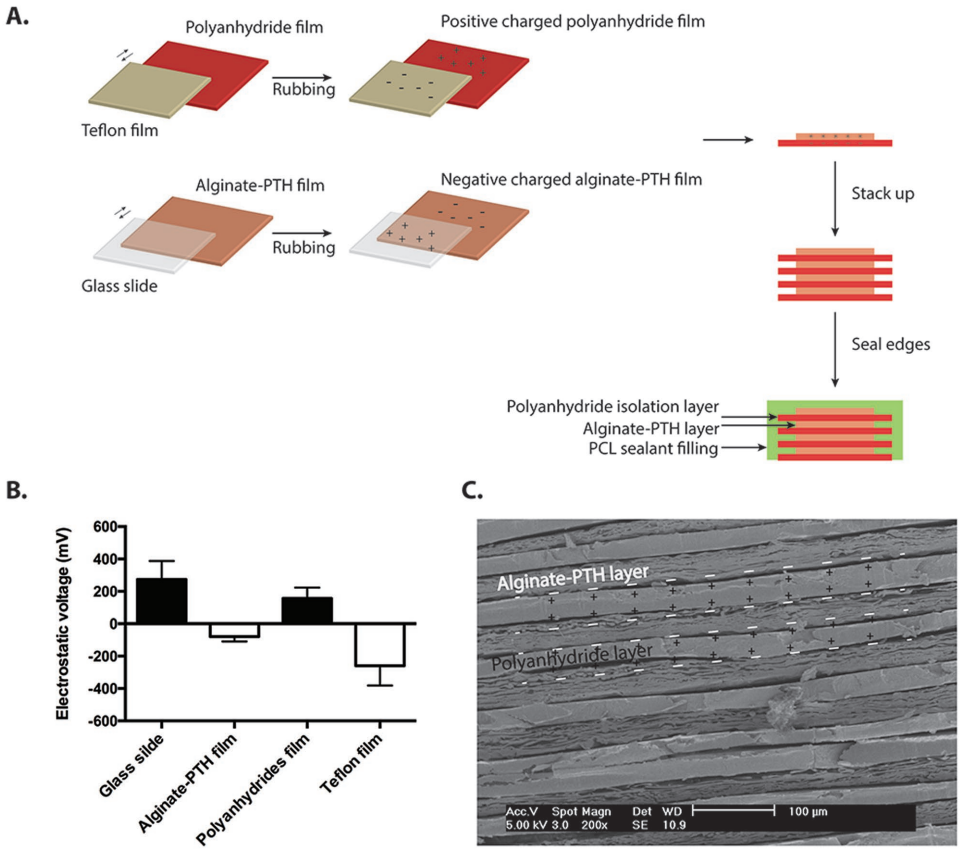

Figure 2. The illustration of the rubbing, stacking, and sealing process to fabricate the pulsatile release device. A) The fabrication process of a multi-pulse delivery device via electrostatic-assisted layer-by-layer stacking technique. B) The electrostatic potential of the different layers after the rubbering process. C) A cross-sectional SEM micrograph of the multilayer pulsatile release device.

then stacked into a 21-bilayer structure. This technique enabled close contact between drug layers and isolation layers and eliminated air gaps (Figure 2C). Constructively, the drug layers were designed to be smaller than the isolation layers in diameter, preventing possible contact between adjacent drug layers, which could lead to leakage of drug between layers. The side and the bottom of the device were sealed with polycaprolactone (PCL), a slow biodegrading polymer,[28] thus allowing unidirectional drug release from the top only.

The pulsatile release profile was preprogrammed by modulating the chemical composition and physical thickness of the isolation PA layer. The poly(SA-CPP) (sebacic acid (SA) and 1,3-bis (*p*-carboxyphenoxy) propane (CPP)) has been used as components of FDA-approved medical devices in human clinical application.[29] However, due to the hydrophobicity of the poly(SA-CPP), the hydrolytic degradation usually takes too long for an ideal pulsatile release profile. Therefore, we incorporated polyethylene glycol (PEG) segments into the poly(SA-CPP) and prepared a three-component PA (poly(SA-CPP-PEG)) by condensation polymerization as described previously.[26] Nuclear magnetic resonance (NMR) spectroscopy confirmed the successful synthesis as the spectrum showed a set of typical poly(SA-CPP-PEG) peaks (Figure S2, Supporting Information). Scanning electron microscopy (SEM) was used to examine the PA degradation. The cross section of the uneroded polymer was uniform, while there were evident pores in eroded portions of the treated samples (Figure S3, Supporting Information). The erosion front moving with time was an indication of surface erosion. The PA containing more PEG segments exhibited a faster erosion rate than those containing fewer PEG segments. It was also observed that the eroded surface roughness increased with increasing PEG content of the PA. The new PEG-containing PA retained the surface erosion properties of the poly(SA-CPP) while imparting a large range of tunable erosion rate.

The "dissolution time" of the surface erosion polymer layer is proportional to the thickness of the layer.[5] Therefore, the thickness of each isolation layer can be adjusted to achieve desired time intervals between adjacent pulses of drug release. PA isolation layers of varying thickness (50, 100, and 200 µm) were used to assemble the multilayer devices, all of which were able to deliver 21 pulses of protein but with different durations (**Figure 3**A–C). The average time interval between adjacent pulses exhibited a linear relation with the thickness of isolation layer (Figure 3D).

As also demonstrated, the degradation rate of the three-component PA escalated with increasing PEG content. Varying the chemical composition and the layer thickness allowed us to preprogram the release kinetics to target the entire three week therapeutic window. The device made of 50 µm PA (weight ratio: SA-CPP-PEG = 80-20-2) could release 1 pulse per day and

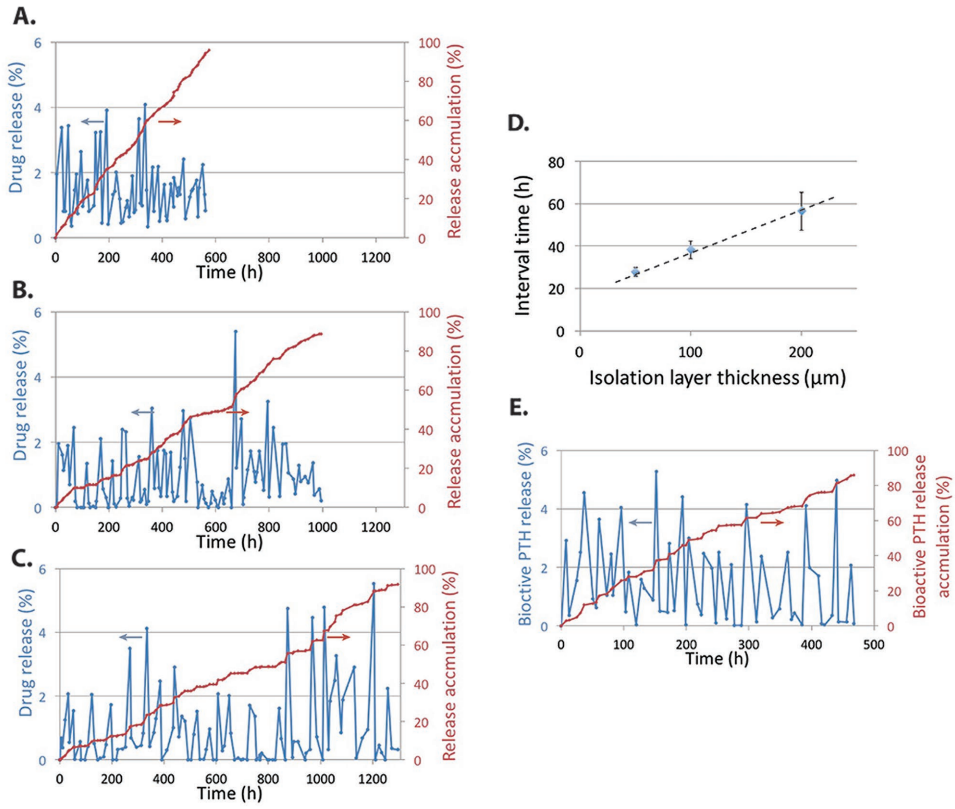

Figure 3. In vitro pulsatile drug release profiles. BSA release from devices of various isolation layer thickness. A) 50; B) 100; C) 200 μm. D) The average time interval between adjacent pulses exhibited linear relation with the thickness of isolation layer. E) Bioactive PTH released in vitro from a pulsatile drug delivery device with 50 μm thick isolation layers.

was therefore chosen for PTH–PTH loading. Release kinetics of bioactive PTH was determined using an adenylyl cyclase stimulation and cAMP binding assay,[30] which showed that 21 pulses of bioactive PTH were achieved over three weeks, and that released PTH retained around 80% bioactivity (Figure 3E).

2.1.2. Continuous Delivery Device

Another device, with identical shape, size, and component materials to those of the pulsatile release device, was engineered to deliver the same total amount of PTH but in a continuous manner. This continuous device was designed to serve as a control device in order to determine the in vivo therapeutic effect in response to different PTH delivery patterns. We employed a double emulsion method to prepare drug-encapsulated PA microspheres, which were then compressed into a disk of the same shape and size as the pulsatile device (**Figure 4**A).

We achieved linear continuous release of the model protein (BSA) (Figure 4B). Interestingly, unlike most microsphere-based continuous delivery systems (such as poly(lactic-co-glycolic acid), polylactic acid),[31] there was no burst release and the sustained release of BSA from the new continuous release device was linear with release time. SEM observation showed that the uneroded PA particles were spherical in shape with smooth surfaces, and that during degradation in phosphate buffered saline (PBS), the size of the particles decreased, the particles lost the spherical shape, and fused together (Figure S3, Supporting Information). Instead of being porous throughout the particles, which would likely lead to a burst drug release, the surface erosion property of the PA resulted in the degradation only on the surface, thus enabling the steady linear drug release from the microspheres. In addition, the unidirectional device design also contributed to the linear delivery kinetics, since the PBS only eroded spheres on the exposed disk surface and penetrated in a downward direction as the downmoving surface degraded.

The release kinetics of the linear release device could also be modulated by varying the chemical composition of the PA. The drug release profiles showed that the drug release rate increased with increasing hydrophilic PEG segments (Figure 4B). The device made of the highest PEG content (10%) PA released 100% of the drug in 400 h, whereas the device made of no PEG content PA only released 50% of the drug in 400 h. The PA (80-20-2) device was able to release 90% of the drug in 21 d, which was the targeted three week window of anabolic PTH treatment. Therefore, PTH was encapsulated into PA (80-20-2) microspheres and bioactive PTH was measured using the adenylyl cyclase stimulation and cAMP binding assay. The bioactive PTH was released from the device following a linear release profile with bioactivity not statistically different from that of released PTH from the pulsatile device (Figure 3C).

Both types of devices were constructed with the same components: the drug (PTH), isolation or encapsulation materials

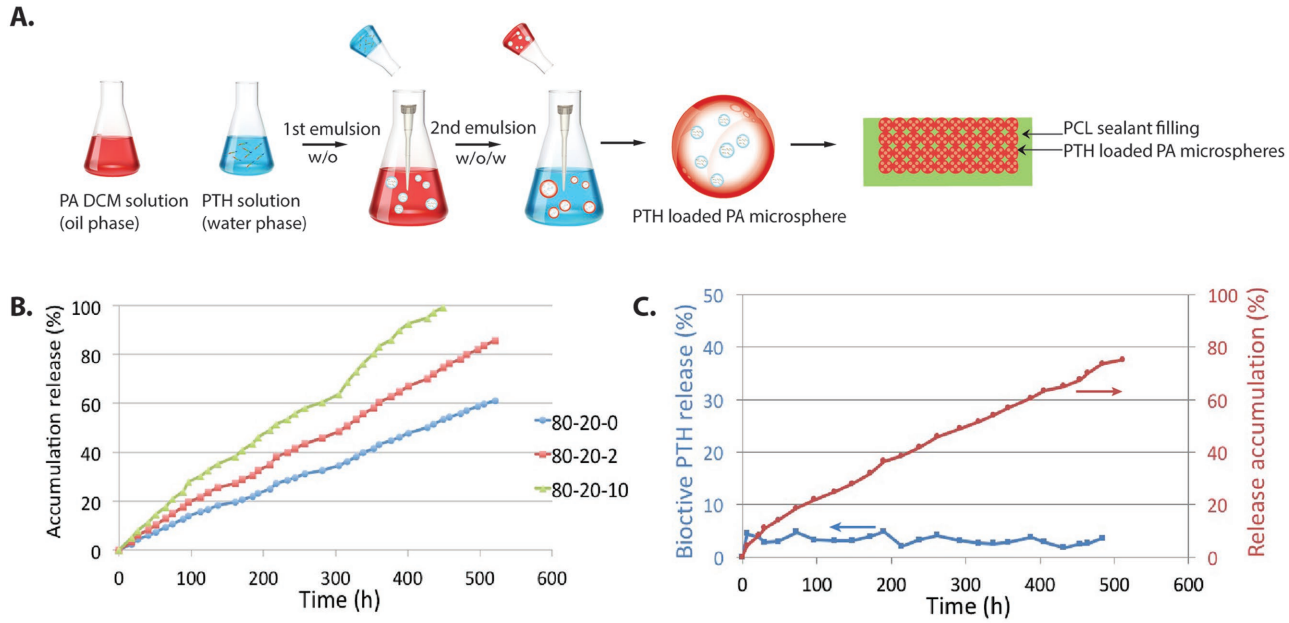

Figure 4. Continuous release device fabrication and release profiles. A) Schematic illustration of the fabrication process of the PA microspheres via double emulsion method and the construction of the continuous delivery device. B) In vitro release of BSA from continuous drug delivery device with different PAs. C) In vitro bioactive PTH released from continuous drug delivery device with PA (80/20/2).

(PA), and sealant material (PCL) but the distribution of PTH in the devices was different, resulting in distinct release profiles. In the pulsatile device, PTH was isolated by PA in a layer-by-layer structure, wheras PTH was confined in microdomains that were uniformly distributed throughout the continuous device. The surface erosion property of the PA (SA-CPP-PEG) is essential to achieve the two types of the release kinetics. In the pulsatile device, it enabled the daily-pulsed release because the PBS could only erode one isolation layer before releasing one drug layer. In the continuous device, the surface erosion property enabled the PTH release from microspheres on the exterior surface then gradually from those inside the device, resulting in the linear continuous drug release. Moreover, the structural tunability of this three-component PA enabled a broad range of interval time in the pulsatile device or release duration time in the continuous device.

2.2. In Vivo Actions of Engineered PTH Release on Bone

Current PTH administration relies on injection but comparing different PTH release kinetics from controlled delivery system has not yet been studied. PTH has been shown to promote bone formation in vivo via a net anabolic action, however it inhibits osteoblast differentiation and mineralization in vitro, indicating that the in vivo environment cannot be replicated using in vitro model.[32] Hence, in vivo models are a necessity to determine PTH's optimal delivery mode from the engineered devices. With the PTH release devices fabricated and function confirmed, the PTH devices were evaluated in vivo to compare the pulsatile and continuous release modes in terms of anabolic effects on bone. Both pulsatile and continuous devices (4 mm in diameter and ≈1.6 mm in thickness) (Figure S5B, Supporting Information) were loaded with equal amounts of PTH and implanted subcutaneously in mice. Three weeks later, the tibia, vertebrae, and blood serum were collected and analyzed.

MicroCT (μCT) evaluation showed that PTH released from the devices had obvious effects on the tibiae. The 3D reconstruction (**Figure 5**A) and the quantitative analysis (Figure 5B,C) showed that the pulsatile PTH release significantly increased trabecular bone volume and cortical bone thickness, while the continuous PTH release acted in the opposite way and decreased both trabecular bone volume and cortical bone thickness. Vertebral bone turnover and the osteoclastic response were examined using hematoxylin and eosin (H&E) staining and tartrate-resistant acid phosphatase (TRAP) staining (**Figure 6**A). Quantitative analysis of the bone area ratio showed that pulsatile PTH significantly increased bone area, while continuous PTH significantly decreased bone area compared to controls (Figure 6B). The serum bone formation marker (procollagen *I* intact *N*-terminal propeptide (PINP)) level was measured using an enzyme-linked immunosorbent assay (ELISA) and showed that the PINP levels were significantly elevated in the pulsatile PTH group (Figure 6C).

Interestingly, TRAP staining of the vertebrae showed that both PTH pulsatile and continuous delivery led to an increased number of TRAP-positive osteoclasts (OSCs) per bone perimeter (Figure 6D,E), but the serum bone resorption marker TRAP 5b level was significantly higher only for continuous PTH release (Figure 6F).

These in vivo results indicated that while delivering the same amount of PTH, the pulsatile release device enhanced bone growth through increasing bone remodeling evidenced by an increase in bone formation marker PINP and enhanced osteoclast numbers, while continuous release induced bone resorption through enhanced osteoclast activity. The systemic

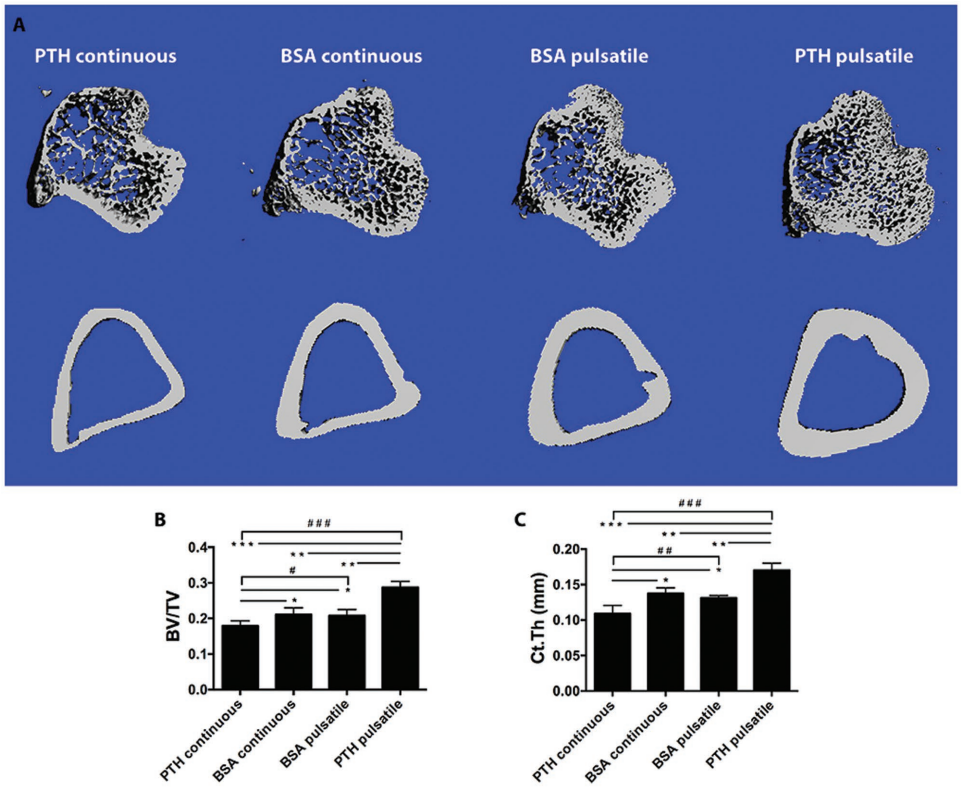

Figure 5. The mouse tibial bone analysis after PTH release using the pulsatile and continuous releasing devices, respectively. A) Representative µCT reconstruction of trabecular bone (top) and cortical bone (below) of the mouse tibias from different treatment groups. B) Trabecular bone volumes. C) Cortical bone thickness. $n = 5–7$ per group, $^{*}P < 0.05$, $^{**}P < 0.005$, $^{***}P < 0.001$, $\#P < 0.05$, $\#\#P < 0.005$, $\#\#\#P < 0.001$.

pulsatile PTH release was found to be superior in terms of anabolic action in bone and significantly strengthened bone systemically after three weeks, so such delivery method could potentially reduce the treatment duration from two years to a significantly short duration.

2.3. Devices' Biodegradability and Biocompatibility

It has always been a question whether degradation byproducts (such as monomers, acids) of a biodegradable polymer result in toxicity and negative effects. The components (SA-CPP and PEG) of PA used in this study have been used as components of FDA-approved medical devices in the human body. The degradation products of the PA copolymer are similar to those of the two components, which potentially have similar biocompatibility.

To help determine biocompatibility, we examined the pH value change during the degradation of the PA devices in vitro and the body response to the implants in vivo. The pH value of the PBS medium, in which devices were immersed, remained about 6.8, close to neutral pH 7, over time as the devices degraded. There was no significant difference between pulsatile and continuous devices (Figure S4A, Supporting Information) since the same amounts of PA were used to fabricate the two types of devices. The in vivo body response to the devices was evaluated using histological analysis of the devices explanted three weeks after subcutaneous implantation. Most parts of the devices had been degraded, leaving the slow degrading sealant shell of PCL (Figure S4B, Supporting Information), which would degrade eventually as reported earlier.[28] H&E staining was performed to assess inflammation at the implant sites in vivo (Figure S4C,E, Supporting Information). The devices were mainly surrounded by granulation tissue composed mostly of macrophages and lymphocytes and partial encapsulation by a fibrovascular connective tissue wall was noted. The inflammatory infiltrate was localized to the area surrounding the devices with limited extension into the adjacent adipose tissue. Overall, all the materials (alginate, PA, and PCL) used to construct the delivery devices are biocompatible and biodegrable. Subcutaneous implanted devices degraded in vivo and resulted in an encapsulation of the materials with minimal acute inflammation.

3. Conclusions

Implantable and biodegradable long-term pulsatile and continuous PTH delivery devices were designed to investigate the effects of PTH delivery patterns on systemic bone therapy. The pulsatile device was preprogrammed to deliver daily pulses of bioactive PTH and the continuous device to deliver bioactive

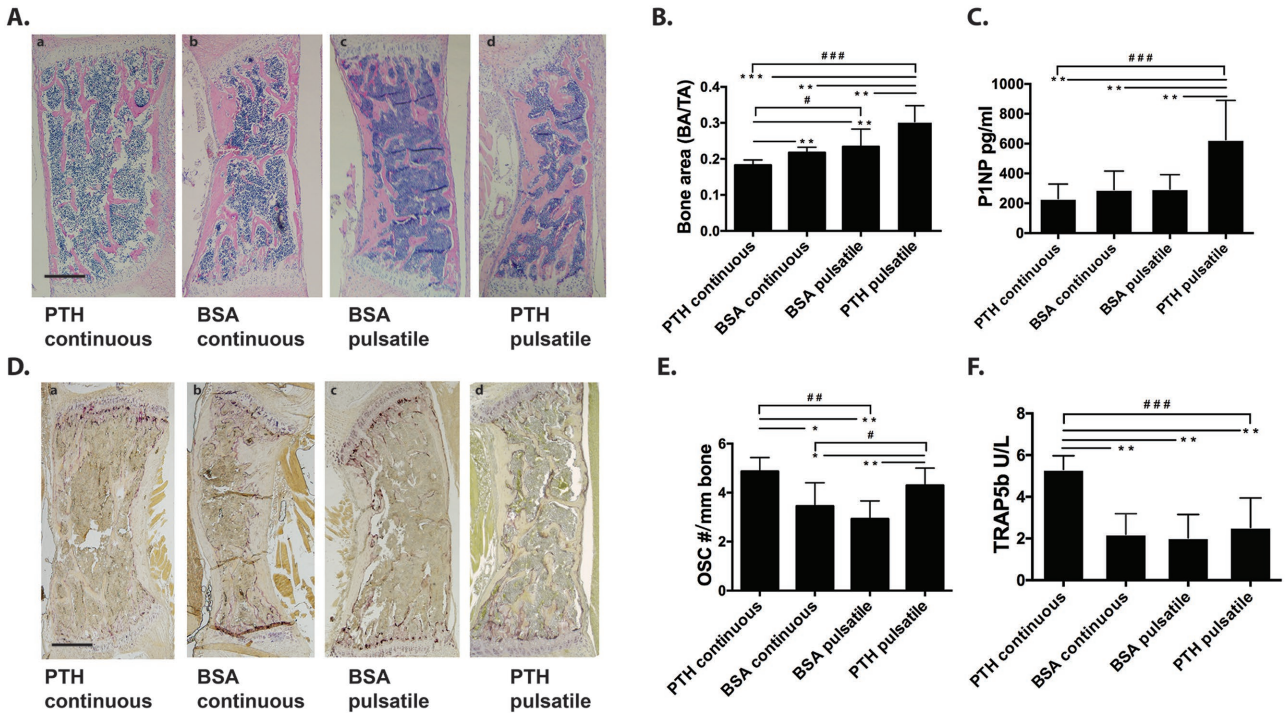

Figure 6. Mouse vetebral bone response to pulsatile and continuous PTH releases. A) Representative H&E staining of vertebrae of different PTH delivery groups. B) Vertebral bone area/tissue area analyzed by histomorphometry. C) Serum PINP level measured by PINP ELISA. D) Representative TRAP staining of vertebrae of different PTH delivery groups. E) Osteoclast (OSC) numbers per bone perimeter. F) Serum TRAP5b level measured by ELISA; pulsatile groups: $n = 9$–12 per group, continuous groups: $n = 6$–9 per group, $^{*}P < 0.05$, $^{**}P < 0.005$, $^{***}P < 0.001$, $^{\#}P < 0.05$, $^{\#\#}P < 0.005$, $^{\#\#\#}P < 0.001$. Scale bar: 0.5 mm (A) and (D).

PTH in a linear manner for three weeks. We demonstrated that systemic pulsatile PTH release was able to increase bone via enhancing bone remodeling, whereas the continuous PTH release resulted in bone resorption via elevated osteoclast resorption activity. The biodegradable pulsatile PTH delivery device has the potential to be a patient-friendly PTH therapy, which could be administered only once (implantation) instead of daily injection. In addition, the device is biodegradable and resorbable in vivo, eliminating the need of removal surgery. Beyond the PTH delivery application, we expect the platform (continuous and pulsatile devices) to be useful in fundamental and translational studies on how temporal effects and release patterns of biomolecules regulate cell fate, tissue development, and regeneration.

4. Experimental Section

Fabrication of the Pulsatile PTH Delivery Device: Three-component PAs composed of SA, CPP, and poly(ethylene glycol) (PEG, $M_w = 1000$) were synthesized as previously reported.[26] ^{1}H NMR (400 MHz, CDCl3) confirmed the synthesis of the PA: PEG (3.4–3.8 ppm), CPP (6.9 and 8.0 ppm), and SA (1.4–2.2 ppm). The PA was melted and compressed into layers of various thicknesses with error ≤10 µm. The PA layers were punched into disks of desired size (3 mm in diameter) as isolation films. BSA or PTH (1-34) (Bachem Bioscience Inc., Torrance, CA) was mixed with alginate in a 1:1.67 weight ratio. The mixture was dissolved in distilled water and the solution was cast into a film and freeze-dried for 1 d. The films were then punched into disks (2 mm in diameter). The PA films were rubbed with a Teflon film to generate positive surface charge and the alginate-PTH films were rubbed with a glass slide to generate negative surface charge. One piece of the PA film and one piece of drug film attracted each other to form one bilayer. The 21 bilayers were stacked and then sealed using a 35% w/v PCL/dichloromethane (DCM) solution, leaving the top unsealed thus allowing one-direction erosion (from top to bottom). The device was vaccum dried for 3 d.

Film Surface Characterization: 10% w/v PA/DCM solution or alginate-PTH aqueous solution was spin coated onto the gold substrate. KPFM (Bruker NanoMan atomic-force microscopy (AFM)) equipped with a conductive tip was used to map the surface potential in tapping mode and the data were analyzed with software (Nanoscope) equipped with the AFM. The drug layer was rubbed with a glass side and the PA was rubbed with a Teflon layer. The electrostatic voltages of the layers (Teflon, glass side, PA layer, and drug layer) were measured using a noncontact static meter (Electro-Tech Systems Static Meter Model 200).

Fabrication of Continuous PTH Delivery Device: To fabricate the continuous PTH release device, we employed the double emulsion method to prepare drug-encapsulated PA microspheres, which were then compressed into disks. Briefly, BSA (control protein) or PTH was dissolved in distilled water with 0.1 wt% gelatin. The drug solution was emulsified in a 10% w/v PA DCM solution, using a probe sonicator at an output power of 10 W (Virsonic 100, Cardiner, NY) for 10 s over an ice bath to first form a water-in-oil (w/o) emulsion. The w/o emulsion was then gradually added into 20 mL aqueous polyvinyl alcohol solution (1% w/v) under sonication at an output power of 20 W to form a water-in-oil-in-water (w/o/w) double emulsion. The solution was stirred at room temperature for 3 h to evaporate DCM and then centrifuged to collect solid microspheres. The resultant microspheres were washed

with distilled water three times and freeze dried. The microspheres were then compressed into disks and the bottoms and sides of the disks were sealed with a 35% w/v PCL/DCM solution, leaving only the top unsealed. The device was dried under vaccum for 3 d.

In Vitro Drug Release and PTH Bioactivity: The protein-loaded devices were immersed in 1 mL PBS (0.1 M, pH = 7.4) and incubated at 37 °C. After designated times, the medium was collected and replaced with equal amount of fresh PBS. The collected medium was stored at −80 °C until analysis. The amount of released BSA was measured using a MicroBCA protein assay (Pierce, Rockford, IL). In vitro bioactivity of released PTH was determined using the adenylate cyclase stimulation assay and cAMP-binding protein assay.[30] Briefly, human fetal osteoblasts were treated with PTH of known concentrations or with eluent from the PTH delivery devices for designated times in calcium-free and magnesium-free hanks' balanced salt solution containing 0.1% BSA and 1×10^{-3} M isobutylmethylxanthine. After incubation of the treated cells at 37 °C for 10 min, the cAMP in the cells was extracted with ice cold perchloric acid. The cAMP extracts were then neutralized by adding KOH and centrifuged to remove the precipitates. (^{3}H)-cAMP was incubated with standards or unknowns and cAMP-binding protein for 90 min on ice. The unbound (^{3}H)-cAMP was removed by adding dextran-coated charcoal. The samples were then centrifuged and the supernatant of each tube was decanted to a scintillation tube. The radioactivity of the supernatants was determined using a liquid scintillation counter and cAMP levels were calculated using the standard curve.

In Vivo PTH Effect on Bone: All animal procedures were carried out under the guidelines of and were approved by the Institutional Animal Care and Use Committee of the University of Michigan. Pulsatile or continuous PTH delivery devices were implanted into subcutaneous pockets created from a midline incision on the backs of C57B6 mice (The Jackson Laboratory, Bar Harbor, ME) at postnatal d 10. Three weeks after implantation, the mice were euthanized and whole blood was obtained by intracardiac blood draw, serum separated and kept frozen until biochemical assays were performed. The serum TRAP5b and PINP immunoassays were performed per manufacturer's protocols. 3D analyses of mice tibiae were performed using μCT as previously described.[33] Briefly, formalin fixed tibiae were embedded in 1% agarose and placed in a 19 mm diameter tube and scanned over their entire length using a μCT system (μCT100 Scanco Medical, Bassersdorf, Switzerland). Scan settings were 12 μm voxel size, medium resolution, 70 kVp, 114 μA, 0.5 mm AL filter, and an integration time of 500 ms. Trabecular bone parameters were measured over 50 slices using an 180 mg cm^{-3} hydroxyapatite (HA) threshold beginning 15 slices distal to the growth plate; cortical bone parameters were measured over 30 slices beginning 250 slices proximal to the tibia–fibular joint using a 280 mg cm^{-3} HA threshold. The trabecular bone volume and cortical bone thickness (Ct.Th) were quantified using the manufacturer's evaluation software (Scanco μCT 100). Mice vertebrae were also harvested for histological analyses. Histomorphometric analyses were performed as previously described.[34] Briefly, after fixation and decalcification, paraffin-embedded tibiae and vertebrae were cut (5 μm), stained with hematoxylin and eosin, and bone areas measured using a computer-assisted histomorphometric analyzing system (Image-Pro Plus version 4.0; Media Cybernetics, Inc., Silver Spring, MD). TRAP staining was performed using the Leukocyte Acid Phosphatase Assay (Sigma) following the manufacturer's protocol.

Statistics: All P values were calculated by an unpaired, one-way ANOVA test using GraphPad InStat software (GraphPad). *P* values were two-tailed and $P < 0.05$ was considered statistically significant. All data are means ± SD.

Supporting Information

Supporting Information is available from the Wiley Online Library or from the author.

Acknowledgements

This work was supported by DOD (W81XWH-12-2-0008) and the National Institutes of Health (NIDCR DE022327). M.D., A.J.K., L.K.M., and P.X.M. designed experiments. M.D., A.J.K., and T.D. performed experiments and analyzed data. M.D. and P.X.M wrote the manuscript.

Received: August 11, 2016
Revised: November 1, 2016
Published online: December 8, 2016

[1] a) B. P. Timko, K. Whitehead, W. Gao, D. S. Kohane, O. Farokhzad, D. Anderson, R. Langer, *Annu. Rev. Mater. Res.* **2011**, *41*, 1; b) S. Mitragotri, P. A. Burke, R. Langer, *Nat. Rev. Drug Discov.* **2014**, *13*, 655; c) B. Chertok, M. J. Webber, M. D. Succi, R. Langer, *Mol. Pharmaceutics* **2013**, *10*, 3531.

[2] a) M. Sokolsky-Papkov, K. Agashi, A. Olaye, K. Shakesheff, A. J. Domb, *Adv. Drug Delivery Rev.* **2007**, *59*, 187; b) J. Shi, A. R. Votruba, O. C. Farokhzad, R. Langer, *Nano Lett.* **2010**, *10*, 3223.

[3] a) R. M. Neer, C. D. Arnaud, J. R. Zanchetta, R. Prince, G. A. Gaich, J.-Y. Reginster, A. B. Hodsman, E. F. Eriksen, S. Ish-Shalom, H. K. Genant, O. Wang, D. Mellström, E. S. Oefjord, E. Marcinowska-Suchowierska, J. Salmi, H. Mulder, J. Halse, A. Z. Sawicki, B. H. Mitlak, *N. Engl. J. Med.* **2001**, *344*, 1434; b) D. W. Dempster, F. Cosman, E. S. Kurland, H. Zhou, J. Nieves, L. Woelfert, E. Shane, K. Plavetić, R. Müller, J. Bilezikian, R. Lindsay, *J. Bone Miner. Res.* **2001**, *16*, 1846.

[4] a) L. Qin, L. J. Raggatt, N. C. Partridge, *Trends Endocrinol. Metab.* **2004**, *15*, 60; b) C. A. Frolik, E. C. Black, R. L. Cain, J. H. Satterwhite, P. L. Brown-Augsburger, M. Sato, J. M. Hock, *Bone* **2003**, *33*, 372; c) D. W. Dempster, F. Cosman, M. A. Y. Parisien, V. Shen, R. Lindsay, *Endocr. Rev.* **1993**, *14*, 690.

[5] X. Liu, G. J. Pettway, L. K. McCauley, P. X. Ma, *Biomaterials* **2007**, *28*, 4124.

[6] a) Z.-G. Gao, H. D. Fain, N. Rapoport, *J. Controlled Release* **2005**, *102*, 203; b) P. Anilkumar, E. Gravel, I. Theodorou, K. Gombert, B. Thézé, F. Ducongé, E. Doris, *Adv. Funct. Mater.* **2014**, *24*, 5246.

[7] a) G. Wu, A. Mikhailovsky, H. A. Khant, C. Fu, W. Chiu, J. A. Zasadzinski, *J. Am. Chem. Soc.* **2008**, *130*, 8175; b) S. J. Leung, X. M. Kachur, M. C. Bobnick, M. Romanowski, *Adv. Funct. Mater.* **2011**, *21*, 1113.

[8] a) J. Ge, E. Neofytou, T. J. Cahill, R. E. Beygui, R. N. Zare, *ACS Nano* **2012**, *6*, 227; b) Y. Wang, M. S. Shim, N. S. Levinson, H.-W. Sung, Y. Xia, *Adv. Funct. Mater.* **2014**, *24*, 4206.

[9] a) S.-H. Hu, T.-Y. Liu, D.-M. Liu, S.-Y. Chen, *Macromolecules* **2007**, *40*, 6786; b) Y. Li, G. Huang, X. Zhang, B. Li, Y. Chen, T. Lu, T. J. Lu, F. Xu, *Adv. Funct. Mater.* **2013**, *23*, 660.

[10] A. C. Grayson, R. Choi, I. S. Tyler, B. M. Wang, P. P. Brem, H. Cima, J. Michael, R. Langer, *Nat. Mater.* **2003**, *2*, 767.

[11] a) A. G. Skirtach, P. Karageorgiev, M. F. Bédard, G. B. Sukhorukov, H. Möhwald, *J. Am. Chem. Soc.* **2008**, *130*, 11572; b) J. Borges, L. C. Rodrigues, R. L. Reis, J. F. Mano, *Adv. Funct. Mater.* **2014**, *24*, 5624.

[12] a) H. Dai, Q. Chen, H. Qin, Y. Guan, D. Shen, Y. Hua, Y. Tang, J. Xu, *Macromolecules* **2006**, *39*, 6584; b) Y.-J. Kim, M. Ebara, T. Aoyagi, *Adv. Funct. Mater.* **2013**, *23*, 5753.

[13] a) Y. Zhu, J. Shi, W. Shen, X. Dong, J. Feng, M. Ruan, Y. Li, *Angew. Chem.* **2005**, *117*, 5213; b) W. Fang, J. Yang, J. Gong, N. Zheng, *Adv. Funct. Mater.* **2012**, *22*, 842.

[14] M. Nazari, M. Rubio-Martinez, G. Tobias, J. P. Barrio, R. Babarao, F. Nazari, K. Konstas, B. W. Muir, S. F. Collins, A. J. Hill, M. C. Duke, M. R. Hill, *Adv. Funct. Mater.* **2016**, *26*, 3244.

[15] B. P. Timko, M. Arruebo, S. A. Shankarappa, J. B. McAlvin, O. S. Okonkwo, B. Mizrahi, C. F. Stefanescu, L. Gomez, J. Zhu, A. Zhu, J. Santamaria, R. Langer, D. S. Kohane, *Proc. Natl. Acad. Sci. USA* **2014**, *111*, 1349.
[16] a) K. Patel, S. Angelos, W. R. Dichtel, A. Coskun, Y.-W. Yang, J. I. Zink, J. F. Stoddart, *J. Am. Chem. Soc.* **2008**, *130*, 2382; b) H. Zhang, J. Fei, X. Yan, A. Wang, J. Li, *Adv. Funct. Mater.* **2015**, *25*, 1193; c) M. J. Cardoso, S. G. Caridade, R. R. Costa, J. F. Mano, *Biomacromolecules* **2016**, *17*, 1347.
[17] a) H. J. Kim, H. Matsuda, H. Zhou, I. Honma, *Adv. Mater.* **2006**, *18*, 3083; b) J. Di, J. Price, X. Gu, X. Jiang, Y. Jing, Z. Gu, *Adv. Healthc. Mater.* **2014**, *3*, 811.
[18] K. Sato, M. Takahashi, M. Ito, E. Abe, J.-I. Anzai, *J. Mater. Chem. B* **2015**, *3*, 7796.
[19] G. Jeon, S. Y. Yang, J. Byun, J. K. Kim, *Nano Lett.* **2011**, *11*, 1284.
[20] T. Hoare, J. Santamaria, G. F. Goya, S. Irusta, D. Lin, S. Lau, R. Padera, R. Langer, D. S. Kohane, *Nano Lett.* **2009**, *9*, 3651.
[21] R. Farra, N. F. Sheppard, L. McCabe, R. M. Neer, J. M. Anderson, J. T. Santini, M. J. Cima, R. Langer, *Sci. Transl. Med.* **2012**, *4*, 122ra21.
[22] G. Wei, G. J. Pettway, L. K. McCauley, P. X. Ma, *Biomaterials* **2004**, *25*, 345.
[23] a) G. J. Pettway, J. A. Meganck, A. J. Koh, E. T. Keller, S. A. Goldstein, L. K. McCauley, *Bone* **2008**, *42*, 806; b) N. S. Datta, G. J. Pettway, C. Chen, A. J. Koh, L. K. McCauley, *J. Bone Miner. Res.* **2007**, *22*, 951.
[24] G. J. Pettway, A. Schneider, A. J. Koh, E. Widjaja, M. D. Morris, J. A. Meganck, S. A. Goldstein, L. K. McCauley, *Bone* **2005**, *36*, 959.
[25] J. D. Bashutski, R. M. Eber, J. S. Kinney, E. Benavides, S. Maitra, T. M. Braun, W. V. Giannobile, L. K. McCauley, *N. Engl. J. Med.* **2010**, *363*, 2396.
[26] S. Hou, L. K. McCauley, P. X. Ma, *Macromol. Biosci.* **2007**, *7*, 620.
[27] a) D. Verma, M. S. Desai, N. Kulkarni, N. Langrana, *Mater. Sci. Eng., C* **2011**, *31*, 1741; b) W. Melitz, J. Shen, A. C. Kummel, S. Lee, *Surf. Sci. Rep.* **2011**, *66*, 1.
[28] H. Sun, L. Mei, C. Song, X. Cui, P. Wang, *Biomaterials* **2006**, *27*, 1735.
[29] K. E. Uhrich, S. M. Cannizzaro, R. S. Langer, K. M. Shakesheff, *Chem. Rev.* **1999**, *99*, 3181.
[30] H.-L. Chen, B. Demiralp, A. Schneider, A. J. Koh, C. Silve, C.-Y. Wang, L. K. McCauley, *J. Biol. Chem.* **2002**, *277*, 19374.
[31] a) J. Panyam, V. Labhasetwar, *Adv. Drug Delivery Rev.* **2003**, *55*, 329; b) J. M. Anderson, M. S. Shive, *Adv. Drug Delivery Rev.* **2012**, *64*, 72.
[32] a) L. K. McCauley, A. J. Koh, C. A. Beecher, Y. Cui, T. J. Rosol, R. T. Franceschi, *J. Cell. Biochem.* **1996**, *61*, 638; b) R. Gopalakrishnan, H. Ouyang, M. J. Somerman, L. K. McCauley, R. T. Franceschi, *Endocrinology* **2001**, *142*, 4379.
[33] S. W. Cho, F. Q. Pirih, A. J. Koh, M. Michalski, M. R. Eber, K. Ritchie, B. Sinder, S. Oh, S. A. Al-Dujaili, J. Lee, K. Kozloff, T. Danciu, T. J. Wronski, L. K. McCauley, *J. Biol. Chem.* **2013**, *288*, 6814.
[34] A. J. Koh, C. M. Novince, X. Li, T. Wang, R. S. Taichman, L. K. McCauley, *Endocrinology* **2011**, *152*, 4525.